Hydrology and
Earth System
Sciences

Open Access

A model of hydrological and mechanical feedbacks of preferential fissure flow in a slow-moving landslide

D. M. Krzeminska[1], **T. A. Bogaard**[1], **J.-P. Malet**[2], **and L. P. H. van Beek**[3]

[1]Department of Water Management, Delft University of Technology, P.O. Box 5048, 2600 GA Delft, the Netherlands
[2]Institut de Physique du Globe de Strasbourg, UMR7516, CNRS, Université de Strasbourg, Ecole et Observatoire des Sciences de la Terre, 5 rue Descartes, 67084 Strasbourg, France
[3]Department of Physical Geography, Utrecht University, UCEL, P.O. Box 80115, 3508 TC, Utrecht, the Netherlands

Correspondence to: D. M. Krzeminska (d.m.krzeminska@tudelft.nl)

Abstract. The importance of hydrological processes for landslide activity is generally accepted. However, the relationship between precipitation, hydrological responses and movement is not straightforward. Groundwater recharge is mostly controlled by the hydrological material properties and the structure (e.g., layering, preferential flow paths such as fissures) of the unsaturated zone. In slow-moving landslides, differential displacements caused by the bedrock structure complicate the hydrological regime due to continuous opening and closing of the fissures, creating temporary preferential flow paths systems for infiltration and groundwater drainage. The consecutive opening and closing of fissure aperture control the formation of a critical pore water pressure by creating dynamic preferential flow paths for infiltration and groundwater drainage. This interaction may explain the seasonal nature of the slow-moving landslide activity, including the often observed shifts and delays in hydrological responses when compared to timing, intensity and duration of precipitation.

The main objective of this study is to model the influence of fissures on the hydrological dynamics of slow-moving landslide and the dynamic feedbacks between fissures, hydrology and slope stability. For this we adapt the spatially distributed hydrological and slope stability model (STARWARS) to account for geotechnical and hydrological feedbacks, linking between hydrological response of the landside and the dynamics of the fissure network and applied the model to the hydrologically controlled Super-Sauze landslide (South French Alps).

1 Introduction

The importance of understanding the hydrological system within a landslide is commonly accepted; however, including hydrological processes and their variability in landslide modelling is quite difficult and, therefore, often limited (Bogaard, 2001; Lindenmaier, 2007). The main difficulties stem from spatial and temporal heterogeneity of bedrock geometry, material layering, hydrological material properties and dominant hydrological processes across the landslide (Malet et al., 2005; Krzeminska et al., 2013). This is particularly true when dealing with slow-moving clayey landslides, where the continuous movement of the sliding material results in fissure formation with successive opening and closing of fissure apertures.

Fissures are a special case of macropores with apertures that vary from a few millimetres up to tens of centimetres. For the purpose of this study, we use the term "fissures" to describe geo-mechanically induced cracks that form and propagate as a result of tensile opening, sliding and tearing (induced by soil mass movements). It is important to stress that these fissures are filled or partly filled with reworked material and, therefore, they should be seen as volumes of increased porosity and increased hydraulic permeability, not as open "cracks" (Krzeminska et al., 2012). The vertical cracks resulting from drying – wetting cycles are not considered. Furthermore, we use the term "preferential flow" to refer to rapid water flow bypassing the bulk of the matrix (Beven and German, 1982) occurring through the areas of enhanced water fluxes due to the presence of fissures.

Presence of fissures creates so called "dual permeability" systems that consider the porous medium as two interacting and overlapping, but distinct continuum with water flow occurring in both continua (Gwo et al., 1995; Greco et al., 2002; Šimůnek et al., 2003; Gerke, 2006; Jarvis, 2007). Fissures influence the time and intensity of groundwater recharge changing the storage capacity of a soil and affect the infiltration processes of rainfall or snowmelt (Bogaard, 2001; Van Asch et al., 2001; Bievre et al., 2011). Depending on fissure geometry and connectivity between them (Beven and Germann, 1982; McDonnell, 1990; Cameira et al., 2000; Nobles et al., 2004), they may have adverse and beneficial effect on landslide activity (Van Beek and Van Asch, 1999; Fannin et al., 2000; Uchida et al., 2001). An extended fissure network may increase the rate of natural soil drainage and limits the building up of pore water pressure. On the contrary, a dead-end fissure network contributes to maintain high pore water pressures in the surrounding soils, once their storage capacity is exceeded. Moreover, fissures may increase the rate of vertical infiltration and, in consequence, increase the rate of groundwater recharge (McDonnell, 1990; Uchida et al., 2001; Krzeminska et al., 2012, 2013).

The complexity of preferential flow processes, and their high spatial and temporal variability, makes it very difficult to measure the processes in the field and to upscale the information to the catchment scale (Van Asch et al., 2007; Van Schaik, 2010). In hillslope hydrological models preferential flow is commonly incorporated as enhanced vertical infiltration, rapid slope-parallel flow on the bedrock surface or modification of the saturated permeability function (Bogaard, 2002; Beckers and Alila, 2004; Kosugi et al., 2004; Mulungu et al., 2005; Zehe and Blöschl, 2004; Zhang et al., 2006) without accounting for spatial and temporal variation of the preferential flow paths characteristics. Weiler and McDonnell (2007) stressed that incorporation of the spatially dynamic nature of preferential flow systems for conceptualisation and parameterisation of the effect of lateral preferential flow on hillslope hydrology is one of the greatest challenge.

In 1999, Van Beek and Van Asch proposed a spatially distributed physically based model coupling hydrological and stability dynamics, developed in the PCRaster environmental modelling software package. The use of meta-language of PCRaster GIS package provides an expedient way to include and change spatially distributed hydrological and geotechnical parameters. In the subsequent development of the STARWARS model (Van Beek, 2002), fissure flow was introduced in a simpler manner, allowing a fraction of the surface detention, equal the volume of free pore space (i.e., fissures), to bypass the unsaturated matrix and directly recharge the groundwater. In 2005, Malet et al. applied the STARWARS model to the Super-Sauze landslide using the simple bypass flow scheme representing only shallow bypassing flow without fissure – matrix interaction. Krzeminska et al. (2012) included more detailed representation of fissure

flow in STARWARS model. Following a dual-permeability approach (Gerke, 2006; Šimůnek et al., 2003; Jarvis, 2007) they assumed the presence of two overlapping and interacting domains, the matrix and fissures blocks, having their own characteristic and properties (i.e., porosity, hydraulic conductivity) and allowing water flow in both domains.

In this paper, we apply the above model (Krzeminska et al., 2012) to the hydrologically controlled slow-moving Super-Sauze landslide and explicitly take into account the mutual dependence between fissures (their geometry and effectiveness for transmitting the water downslope), hydrology and level of landslide activity. The main objective of this study is to model the influence of fissures on the hydrological dynamics of slow-moving landslides and to formulate a framework to incorporate feedback between fissure flow and stability state into landslide modelling.

2 The STARWARS model – dynamic characteristics of fissure network

2.1 General model description

The STARWARS (Van Beek, 2002) model is a spatially distributed physically based model coupling hydrological and stability dynamics. The model consists of a core model describing the dynamics of saturated and unsaturated flow in the soil and of sub-models that describe related hydrological processes such as interception, transpiration, and snow accumulation and snow melt. The core model represents the soil column, typically consisting of three layers, overlying semi-impervious bedrock.

The fissures network is prescribed by the fractional area covered by fissure (F_{fis}), and mean fissure aperture (a_{fis}) or total number of fissures per cell (N_{fis}). Fissures are considered to be filled with reworked material (no open spaces) and they retain their own water level and soil moisture content (Fig. 1; Krzeminska et al., 2012).

Surface fluxes (infiltration and evaporation) are partitioned between matrix and fissure fraction, proportionally to the fraction area. Following the original process description of the STARWARS model, the vertical unsaturated flow (percolation, Pe) in matrix and fissures domain is gravitational and vertical only, and is controlled by the unsaturated hydraulic conductivity using the relationship of Millington and Quirk (1959) and Farrel and Larson (1972). When the percolation towards the lithic contact exceeds the deep drainage, a groundwater table forms and starts to rise from the bottom of the lowest layer upward. The groundwater level is assumed to be vertically contiguous (for both matrix and fissures fraction). Lateral exchange Γ [m³ h⁻¹] within the cell is possible only between the saturated zones of matrix and fissure fractions ($\Gamma_{Sat,FM/MF}$) and the unsaturated zones of the fissure fraction and the saturated zone of the matrix fraction ($\Gamma_{Unsat, FM}$) when water level in the fissure fraction exceeds

that in the matrix fraction. Lateral flow (Q_{sat}) between cells is described by a bulk flow across the saturated zone that arises from the gradient in the total piezometric head and overall transmissivity (Fig. 1). This flux is resolved in the x- and y-direction and is partitioned over the matrix and fissure domain on the basis of the connectivity of the fissure. The fissure connectivity (C_{fis}) represents the chance for fissures to be connected laterally across adjacent soil columns: it can vary from 0–100 % where 0 % means that there is no connection between the fissures and 100 % means full connectivity. For a complete description of the model the reader is referred to Van Beek (2002) and Krzeminska et al. (2012).

2.2 Hydrological feedback

Hydrological feedback is the mutual dependence between landslide hydrological responses and effectiveness of the fissure network to transport water which increases with soil wetness (Tsuboyama et al., 1994; Noguchi et al., 1999; Sidle et al., 2000). Following the concept presented by Krzeminska et al. (2012), the model accounts for dynamic hydrological feedback between fissure connectivity and the degree of saturation of the soil column (Eq. 1).

$$C_{fis,i} = \qquad\qquad\qquad (1)$$
$$\begin{cases} \frac{C_{fis,max}-C_{fis,min}}{\theta_{E,Sat}-\theta_{E,fc}} \cdot (\theta_{E,i} - \theta_{E,fc}) + C_{fis,min} & \text{for } \theta_{E,i} \geq \theta_{E,fc} \\ C_{fis,min} & \text{for } \theta_{E,i} < \theta_{E,fc} \end{cases}$$

where $C_{fis,i}$ and $\theta_{E,i}$ are fissure connectivity [–] and effective saturation of the matrix [–] at time step i, $C_{fis,min}$ and $C_{fis,max}$ are the minimal and maximal fissures connectivity, set to 0.1 and 0.9, respectively; $\theta_{E,fc} = \theta_{E,pF=2.0}$ is effective saturation at the field capacity [–] and $\theta_{E,sat} = 1$ (full saturation).

2.3 Mechanical feedback

Mechanical feedback is the mutual dependence between fissure geometry and differential displacement observed within landslide. The density and, thus, the volume of the fissures, is an important characteristic determining the influence of fissures on landslide hydrology (Beven and Germann, 1982; McDonnell, 1990; Cameira et al., 2000; Nobles et al., 2004).

As already stated, the vertical cracks resulting from drying – wetting cycles are not considered in this paper and the term "fissures" refers to geo-mechanically induced cracks only. Location and morphology of those fissures correspond to mechanical processes within the landslide. There are three basic modes of fissure propagation: tensile opening, sliding and tearing (Anderson, 2005; Schulson and Duval, 2009). However, it is mainly tensile fracturing that dominates the fissure formation at the free surface of the Super-Sauze landslide (Travelletti and Malet, 2012; Stumpf et al., 2013). The long-term field monitoring and airborne ortho-photo or UAV-based ortho-mosaic analysis (Malet et al., 2002; Malet, 2003; Niethammer et al., 2012) allow for the identifying of the
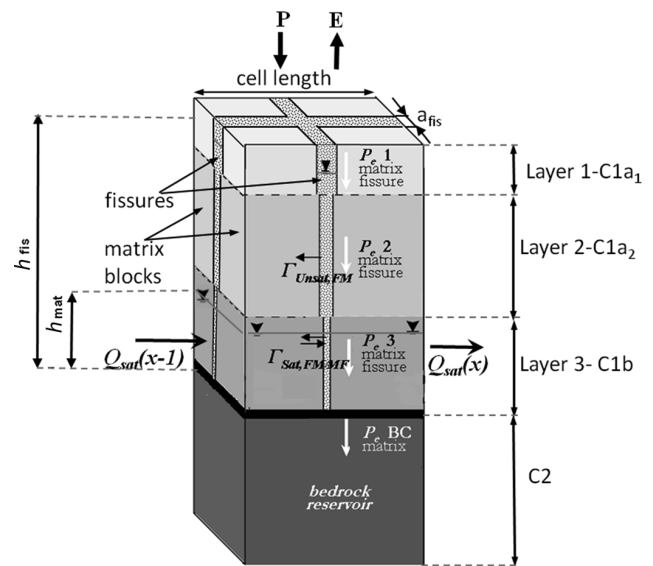

Fig. 1. Schematisation of the hydrological model of the Super-Sauze landslide.

typical surface fissure patterns and their distribution across the landslide. It can be observed that the spatial distribution of fissure patterns is not changing significantly in time despite continuous landslide activity. This indicates strong dependence between the geometry of the stable bedrock, mechanical properties of the sliding material and fissures occurrence (Fig. 4; Niethammer et al., 2012; Walter et al., 2012; Stumpf et al., 2013). Consequently, observed surface fissures are good indicators of local deformation level, that could be extended over the whole soil profile with relatively brittle top soil behaviour (0–1 m) and more ductile behaviour in deeper layers (Stumpf et al., 2013).

Moreover, a significant increase of fissure density can be observed in spring or beginning of summer, which correlates with observed landslide acceleration periods (Malet, 2003). Further development of surface fissure patterns depends on the level of landslide activity (e.g., displacement rates) and meteorological conditions (e.g., precipitation). After the acceleration period, fissures may be filled with some surface deposit and/or (partly) closed due to compaction. During the deceleration period, prolonged dry periods may result in increased brittleness of the upper soil layer and consequently increase in fissure density (Stumpf et al., 2013).

These observations show that temporal changes in fissure volume and density are the result of complex and interacting processes. Here, we present a first attempt to account for dynamically changing fissure volume by correlating fissure density (and, thus, fissure volume) with factor of safety, which is a deterministic measure of slope stability. Factor of safety (f_s) is the ratio between maximum shearing resistance of failure and shear stress and is calculated here with the assumptions of the infinite slope model (Skempton, 1964), which is reasonable for landslides 25 times longer than they

are deep (Milledge et al., 2012). The interaction between cells is neglected and the shear surface is assumed to be equal to the depth of the particular soil column. These assumptions are very efficient for a GIS because calculated stability depends on the attributes of each individual soil column only (Van Asch et al., 1996; Van Beek and Van Asch, 2004). As such, f_s serves here as a proxy for the excess shear stress that cannot be accommodated by a particular soil column and, thus, can lead to soil extension (e.g., appearance and/or extension of shear and tension fissures) or compression (e.g., closing of existing fissures and/or appearance of compression fissures and bulges).

We empirically conceptualised the general relationship between factor of safety and fissure volume. When the soil column is relatively stable ($f_s \gg 1$) there are no, or very limited, fissures present within this soil column. When the stability of the soil column approaches equilibrium limit ($f_s = 1$), more fissures appear and the volume of fissures increases with decreasing f_s. In practice, this means that f_s calculated for a particular cell (soil column) controls the volumes of the domains within this cell (matrix/fissures). This simplified relationship between fissure density (F_{fis}) and factor of safety (f_s) is described with Eq. (2).

$$F_{\text{fis},i} = \qquad\qquad\qquad\qquad\qquad\qquad (2)$$

$$\begin{cases} F_{\text{fis,max}} & \text{for } f_{\text{s},i} < f_{\text{s,min}} \\ \frac{(f_{\text{s,max}} - f_{\text{s},i})}{(f_{\text{s,max}} - f_{\text{s,min}})} \cdot (F_{\text{fis,max}} - F_{\text{fis,min}}) + F_{\text{fis,min}} & \text{for } f_{\text{s,min}} \leq f_{\text{s},i} \leq f_{\text{s,max}} \\ F_{\text{fis,min}} & \text{for } f_{\text{s},i} > f_{\text{s,max}} \end{cases}$$

The $F_{\text{fis,min}}$ and $F_{\text{fis,max}}$ are the upper and lower limit of fissure density. The $f_{\text{s,min}}$ and $f_{\text{s,max}}$ define the range of factor of safety that corresponds to the range of changes in fissure density.

3 Modelling of the Super-Sauze landslide

3.1 Description of the Super-Sauze landslide

The Super-Sauze landslide (Fig. 2a) is a persistently active landslide. It covers $0.17\,\text{km}^2$ of surface and its volume is estimated at approximately $560\,000\,\text{m}^3$ (Travelletti and Malet, 2012). The average slope of the landslide is $25°$. The landslide consists of strongly heterogeneous clayey material (Fig. 2c), reworked blocks and panels of marls at various stages of weathering, clast of all sizes and silty-clay matrix with calcite and moraine blocks (Malet et al., 2003). The preferential water and material pathways are delimited by buried parallel crests and gullies.

From a hydrological and geotechnical point of view, the landslide consists of two superimposed vertical units overlaying the bedrock (Fig. 2b; Malet, 2003; Travalletti and Malet, 2012). A surficial unit (C1) is very active and very wet viscous mud formation of 5 to 9 m thickness, saturated hydraulic conductivity (k_{sat}) ranging from 10^{-4} to $10^{-8}\,\text{m s}^{-1}$ and plasticity index (I_{p}) between 10 and 23. The deeper

unit (C2) is a stiff compact, impervious and stable formation (thickness $= 5\text{–}12\,\text{m}$, $k_{\text{sat}} = 10^{-11}\text{–}10^{-8}\,\text{m s}^{-1}$). The surficial unit (C1) is divided in two secondary units, C1a and C1b, depending on the shape of the paleotopography and hydrological properties, e.g., decreasing the k_{sat} and porosity (n) with depth due to compaction. The soil surface is highly irregular and affected by cracking due to mechanical tension (fissures from around $0.5\,\text{m}$ to more than $1.0\,\text{m}$ deep; Fig. 2d). The heterogeneity of the material and local surface mass movement processes (e.g., small surface mudflow accumulation lobes, local runoff wash deposits) explain important variations of porosity (from 0.33 to 0.49) and vertical hydraulic conductivity (from 10^{-8} to $1.8 \times 10^{-5}\,\text{m s}^{-1}$) over the area (Malet, 2003; Malet et al., 2005).

The landslide kinematics is controlled by hydrology (Malet et al., 2002). The mass movement occurs as a consequence of the rise of groundwater table and, hence, the development of positive pore pressure (Fig. 3b–c). The groundwater originates mostly from rainfall and snow melt infiltration both in the soil matrix and in the fissure system. The activity of the landslide is seasonal and its velocities vary from $0.02\text{–}0.05\,\text{m day}^{-1}$ up to $3.00\,\text{m day}^{-1}$ during acceleration peaks observed in spring season (Fig. 3a–b; Malet et al., 2003; Travelletti et al., 2012).

Based on hydro-geomorphological (Figs. 2b–d and 3c) and kinematical characteristics (Fig. 3a–b), the landslide can be divided into three main units (Fig. 2a; Malet et al., 2005). The "upper unit" characterised by very rapid piezometric response and large groundwater level variations at the event scale (up to $0.5\,\text{m}$) and relatively medium variation at the yearly time scale (0.5 to 1.0 m). The interconnected network of fissures filled or partly filled with loosely packed material is present in this area and provides the paths for fast preferential infiltration. Based on Krzeminska et al. (2013), this unit can be divided in two sub-units (U1 and U2; Fig. 2a) depending on dominant hydrological processes. The "lower unit" (U3) has modest event scale groundwater level fluctuations (0.05 to 0.30 m), but relatively high seasonal variation (0.1–2.5 m). Infiltration processes take place mainly through the matrix since crack systems have limited vertical and horizontal extend. Finally, the "stable unit" (U4) of the landslide characterised by very limited groundwater level fluctuations (centimetres) on both yearly and event time scale.

3.2 Model representation of the Super-Sauze landslide

The geometry, parameterisation and hydrological concepts of the Super-Sauze landslide are a further extension of the work presented by Malet et al. (2005).

The overall geometry of the Super-Sauze landslide has been defined based on 3-D geometrical model of the landslide (Travelletti and Malet, 2012) with the spatial resolution at the pixel of $5 \times 5\,\text{m}$. Spatial representation of the landslide composes of four units corresponding to the hydro-geomorphological units (Fig. 2a). Vertically, landslide body
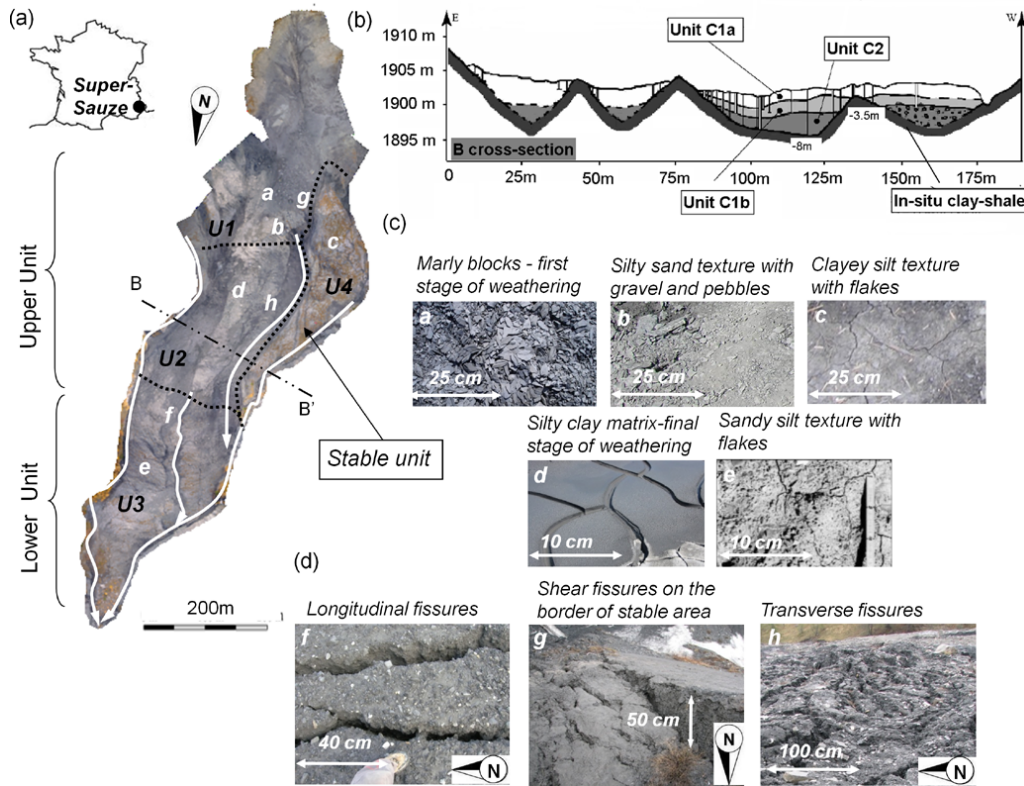
Fig. 2. (a) The Super-Sauze landslide with indicated hydro-geomorphological units (after Malet et al., 2005), the main streams/drainage paths within landslide (white arrows) and location of B-B′ cross section; **(b)** geotechnical structure observed in B-B′; **(c)** soil surface characteristics observed over the landslide area; **(d)** example of fissures formations observed over the landslide area. Pictures taken during filed campaigns in May and July 2008.

is represented by the layers corresponding to C1a and C1b units (Fig. 2b). The maximal depth of C1a is 3 m and of C1b is 9 m. Following the idea of Malet et al. (2005), we defined additional near surface layer (C1a$_1$) with an assumed maximum depth of 1 m. This layer is the most influenced by fissures.

3.3 Fissure fraction characteristics

The maximum fissure fraction ($F_{\text{fis,max}}$) of the near surface unit (C1a$_1$) has been derived from the analysis of the aerial photographs of the landslide from the period of 2007–2008 (Niethammer et al., 2012) and generalised in four zones across the landslide (Fig. 4). Zone 1 (F1) represents areas with no, or very limited, fissures observed at the soil surface. However, there is field evidence for the presence of preferential flow paths in these areas (Krzeminska et al., 2013). Therefore, $F_{\text{fis,max}}$ in F1 is set to be 5 % and $F_{\text{fis,min}}$ is set to be equal to $F_{\text{fis,max}}$ (no mechanical feedback is considered). The $F_{\text{fis,max}}$ and $F_{\text{fis,min}}$ for deeper layers were set arbitrary taking into account that generally the volume of fissures decreases with depth (due to compaction and rheology) and that they should be continuous throughout the vertical profile

(model requirement; Krzeminska et al., 2012). All $F_{\text{fis,max}}$ and $F_{\text{fis,min}}$ values are listed in Table 1.

3.4 Meteorological data

The meteorological data (rain intensity, air temperature, incoming short wave radiation and relative humidity), observed at 0.8 km distance from the landslide, were used to perform model runs. A snowmelt routine based on the degree-day approach was applied. A temperature threshold (T_s) was used to discriminate rainfall from snow fall and a critical temperature (T_m), above which snowmelt occur, was used to govern the melt equation. A vegetation cover is not considered in the model as the landslide has no or very limited vegetation.

3.5 Model calibration and validation

The model was calibrated against observed snow coverage and groundwater level fluctuation over the period of one calendar year (January–December 2007). The initial distributed water level, soil moisture and snow thickness conditions were produced by running the model for one year (2007), for multiple times until a dynamic steady-state was achieved. The time step resolution of the model is 1 h.
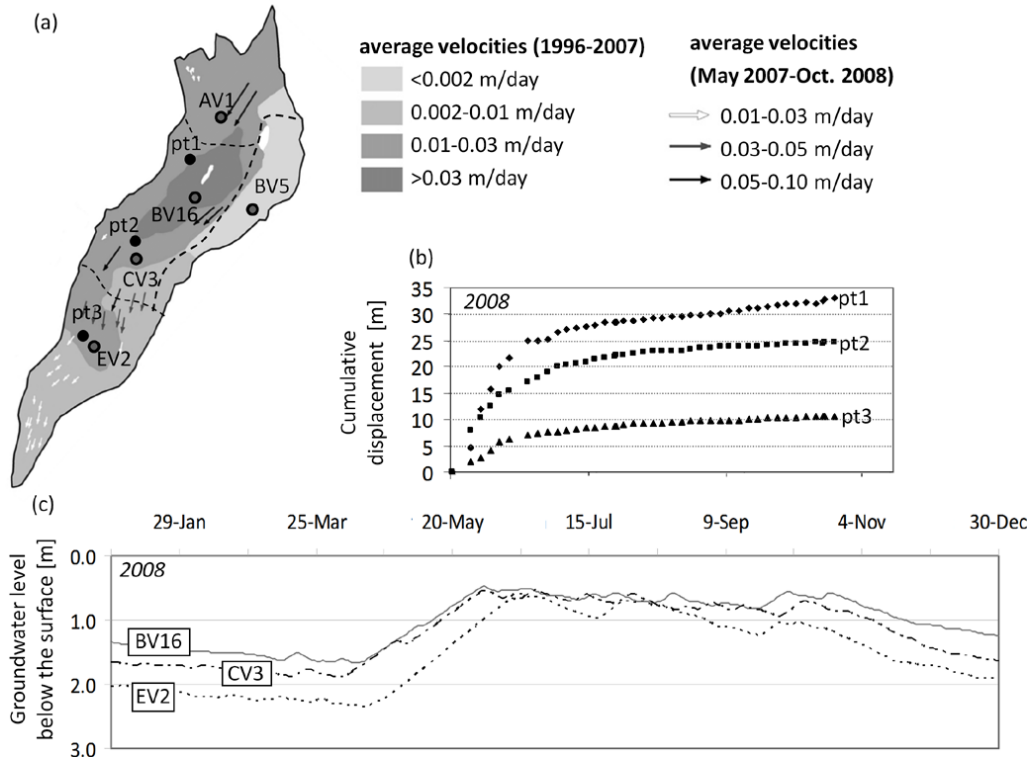
Fig. 3. (a) Horizontal surface displacement observed between May 2007 and October 2008 based on ortho-photo analysis (Niethammer et al., 2012) and long-term average movement velocity map (1996–2007) as reported by Malet et al. (2003); note the location of the piezometers, measurements points of displacement and the hydro-geomorphological units; **(b)** cumulated displacement measured at three points: pt1, pt2 and pt3 (Travelletti et al., 2012); **(c)** groundwater level fluctuation observed at three piezometers (BV16, CV3, EV2) between May 2008 and November 2008.

Table 1. Maximum and minimum fissure fraction as defined per zone and per layer.

	Zone 1		Zone 2		Zone 3		Zone 4	
	$F_{\text{fis,max}}$	$F_{\text{fis,min}}$	$F_{\text{fis,max}}$	$F_{\text{fis,min}}$	$F_{\text{fis,max}}$	$F_{\text{fis,min}}$	$F_{\text{fis,max}}$	$F_{\text{fis,min}}$
Layer 1 (C1a$_1$)	5 %*		10 %	5 %	20 %	10 %	40 %	20 %
Layer 2 (C1a$_2$)	0 %*		5 %	2 %	10 %	2 %	20 %	2 %
Layer 3 (C1b)	0 %*		2 %*		2 %*		2 %*	

* $F_{\text{fis,max}} = F_{\text{fis,min}}$ – no mechanical feedback considered.

A two stage calibration procedure has been applied (Fig. 5). In the first stage, the model including only the hydrological feedback (Krzeminska et al., 2012) was calibrated in order to get estimates of $f_{\text{s,min}}$ and $f_{\text{s,max}}$ needed for introducing mechanical feedback (see Eq. 2). This included the calibration of the "snow pack/snow melt" model and the core hydrological model. The "snow pack/snow melt" model was calibrated against binary "snow-no snow information". The effective parameters that produce the snow cover ($S_{\text{C,sim}}$) duration comparable to the observed one ($S_{\text{C,obs}}$) are: $T'_s = 1\,°\text{C}$ and $T'_m = 6\,°\text{C}$. The liquid water holding capacity of snow pack was set to be constant over time and equal 0.10 and a

day-degree factor equal to $2.5\,\text{mm}\,\text{day}^{-1}\,°\text{C}^{-1}$. It is important to note that the relatively high effective values for T'_s and T'_m are the effect of compensating for local variations in meteorological factors (lapse in temperature, shading and radiation) and diurnal changes in temperature when modelling with a 1 h simulation time step. The same duration of snow cover would be obtained using $T'_s = 1\,°\text{C}$ and $T'_m = 1\,°\text{C}$ with 24 h simulation time step.

Next, the core hydrological model was calibrated. The initial hydrological parameters of matrix and fissure fractions were based on field – measured parameters as reported by Malet et al. (2005) and they were assumed to be equal for
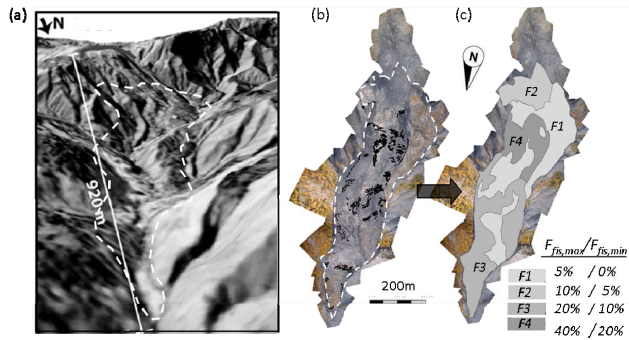
Fig. 4. (a) The DEM of Super-Sauze landslide area from 1956, before the initial failure of the slope with marked current boundary of the landslide. **(b)** The aerial photography (July 2008) with fissures are marked with black lines; **(c)** the implemented fissures zones with defined maximal ($F_{\text{fis,max}}$) and minimal ($F_{\text{fis,min}}$) observed fissure fraction in the surface layer.

the whole landslide. The distinction between parameters for matrix and fissure fraction was made by assuming minimum and maximum measured values being representative for matrix and fissure characteristics, respectively (Table 3). For example, if the range of measured porosity in the field is 0.36 to 0.49 (Malet et al., 2005) then the minimum (0.36) is assumed to represent matrix porosity and maximum (0.49) fissure porosity. Additionally, the hydraulic conductivity of fissure fraction is assumed to be 10 times higher than the one of matrix fraction.

The model was calibrated by changing saturated conductivity ($k_{\text{sat,mat/fis}}$) and porosity ($n_{\text{mat/fis}}$) only. These four parameters were chosen since they show the highest variability when measured in the field and the hydrological model is most sensitive to their variations (see Van Beek, 2002; Malet et al., 2005; Krzeminska et al., 2012). Observed piezometric water levels (see Fig. 2a for the location of the piezometers) were assumed to be the representative for particular units within the landslide (Table 2). The parameters were differentiated per landslide unit (within the range of ±50 % for $n_{\text{mat/fis}}$ and ±100 % for $k_{\text{sat,mat/fis}}$) and adjusted to come to the smallest differences between modelled (h_{sim}) and observed (h_{obs}) groundwater level fluctuations per landslide unit (U1–U4).

The stability sub-model was not calibrated, but the soil strength parameters, cohesion (c) and the angle of friction (φ), were set for the entire landslide in order for the factor of safety per cell (f_s) to oscillate around unity for the most active areas of the Super-Sauze landslide (Fig. 2a). Figure 6a shows the results from the simulation performed with $c' = 8$ kPa and $\varphi' = 25°$. This parameter's set is in agreement with the values presented by Malet (2003) for C1b sub-layer where, according to our conceptualisation, the slip surface is located.
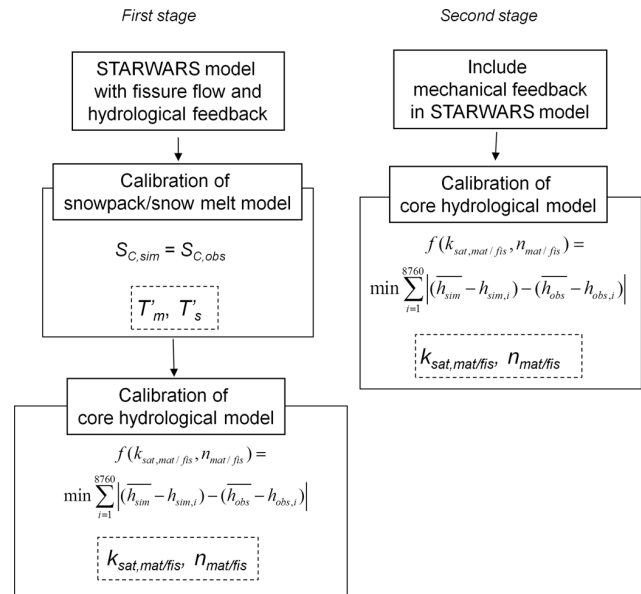

Fig. 5. The calibration procedure.

The upper and lower factor of safety, $f_{\text{s,min}}$ and $f_{\text{s,max}}$ were set to 0.7 and 1.3, respectively, as the simulated values of the annual average factor of safety ($f_{\text{s,av}}$) falls in this range for more than 75 % of landslide area (Fig. 6a).

The second stage of the calibration procedure was based on the simulations performed with both hydrological and mechanical feedbacks. The saturated conductivity ($k_{\text{sat,mat/fis}}$) and porosity ($n_{\text{mat/fis}}$) were again adjusted. Table 3 gives the final calibration results.

At the end, the model including both hydrological and mechanical feedbacks was validated for the year 2008.

4 Simulation results and discussion

Figure 7 presents observed and simulated groundwater level fluctuations over years 2007 (calibration period) and 2008 (validation period). The simulated groundwater level fluctuations representative for particular hydro-geomorphological units were collated with observed piezometric groundwater levels fluctuation (Table 2, Fig. 3). The general range of the groundwater level fluctuation and the timing of the major peaks are well represented by the model. The root-mean-square error (RMSE) between observed and simulated groundwater level variations representative for four units (see Table 3) for the calibration period varies between 0.18 and 0.40 m for the calibration period, and between 0.20–0.44 m for validation period. The differences between observed and modelled groundwater fluctuations mainly stem from the collating of point measurements with area averaged simulated results. During the winter periods and short after the snow melt the difference are also related to inaccuracy of the "snow pack/snow melt" sub-model.
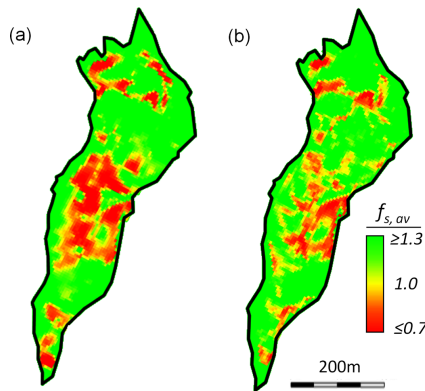
Fig. 6. The annually average factor of safety ($f_{s,av}$) simulated for one year calibration period (2007) with the model **(a)** accounting for hydrological feedback only (first stage of calibration) and **(b)** accounting for both hydrological and mechanical feedbacks (second stage of calibration).

The maximum fissure fraction observed during simulation occurs in July 2007 and the minimum fissure fraction occurs in period of October–November 2007 (Fig. 8). The maximum variation in fissure fraction (ΔF_{fis}) is 13 % and it occurs in the area with the highest fissure fraction (F4) and relatively high landslide activity (Fig. 3a). This behaviour of the fissure fraction is in agreement with what is expected from the field monitoring (Fig. 3b–c): rising groundwater level is associated with growing displacement rate and results in a more extended fissure network.

The model performance regarding the simulation of spatial differences in potential landslide movement was tested by collating the simulated values of factor of safety with observed displacement rate reported by Travelletti et al. (2012) for the year 2008 (Fig. 3b). The modelled distribution of the factor of safety (Fig. 6b) represents the observed Super-Sauze landslide activity (Fig. 3a) quite well: the middle upper part of the landslide is "the most active one" (f_s is the lowest) while the lower part of the landslide is relatively stable (f_s above 1.0 for most of the time during the simulation period) and the western part is the most stable area. However, in the validation period (May–September 2008), there is a 20 days time-lag between modelled decreases in f_s and observed displacement rate. This time lag is also visible between simulated and observed groundwater level variation during the validation period (Fig. 7) and it results from the "snow pack/snow melt" calibration. The simulated time lag can be significantly reduced by changing the effective critical temperature for snow melt for the validation period ($T'_m = 5\,°C$). With this adjustment the simulated spatio–temporal patterns of the factor of safety follow the observed displacement rates very well (Fig. 9). It is interesting to note the differences between the distribution of the annual average factor of safety ($f_{s,av}$) simulated with the model accounting for hydrological feedback only and the model accounting

Table 2. Landslide unit and corresponding measuring points (see also Figs. 2a and 3a).

Unit (Fig. 2a)	Piezometer (Fig. 3a)	Point of displacement measure (Fig. 3a)
U1	AV1	–
U2	BV16 & CV3	pt1, pt2
U3	EV1	pt3
U4	BV5	–

for both hydrological and mechanical feedbacks (Fig. 6a and b). Introduction of dynamically changing fissure volume (in practice changing the porosities and hydraulic conductivity) influences the distribution of water within landslide body (Krzeminska et al., 2012; see also Fig. 10) and, consequently, influences the calculation of the local factor of safety.

In order to study the influence of the implemented dynamic characteristics of the fissure network, $F_{fis}(f_s)$ and $C_{fis}(\theta_E)$, three scenarios were analysed:

- scenario-1 – both hydrological $C_{fis}(\theta_E)$ and mechanical feedbacks are included, $F_{fis}(f_s)$

- scenario-2 – only hydrological feedback ($C_{fis}(\theta_E)$ is included; F_{fis} is assumed to be constant ($F_{fis} = F_{fis,av}$) and $F_{fis,av}$ is estimated based on fissure fraction simulated with scenario-1, averaged over the fissure areas (F1–F4, Fig. 4c) and over one year simulation period;

- scenario-3 – fissure network is not considered, only matrix fraction is present.

Figure 10 shows the difference in groundwater behaviour modelled with three scenarios. The highest differences between the scenarios in simulated groundwater level behaviour can be seen in the middle part of the landslide (U2; Fig. 2a). There are no, or very limited differences observed in groundwater level behaviour within stable unit (U4; Fig. 2a).

In general, the minimum simulated groundwater level (h_{min}; Fig. 10a) is the lowest for scenario-3 (no fissure network included) and the highest for scenario-2 (fissure network with hydrological feedback only). The analogous trend is observed when comparing the annual range of simulated groundwater level fluctuations ($h_{fluctuation}$; Fig. 10b): scenario-3 presents the highest variations of simulated groundwater level and in case of scenarios-2 the simulated groundwater level fluctuations are the lowest. The overall modelled groundwater level, averaged over a one year simulation period (h_{av}), is the highest for scenario-2 and the lowest for scenario-3 (Fig. 10c). The differences between the scenarios are in agreement with the results presented by Krzeminska et al. (2012) for the "simple" landslide representation: introduction of fissure network and accounting for the dynamically changing fissure connectivity resulted in an increase in total average water stored within the landslide.

Table 3. The range of field measured parameters (Malet et al., 2005) and the set of parameters after model calibration.

Parameter	Field measurements	Optimal model parameters	
		Matrix fraction	Fissure fraction
Saturated conductivity – $C1a_1$ [m s^{-1}]	6.10×10^{-6}–1.05×10^{-5}	6.02×10^{-6}	6.02×10^{-5}
Saturated conductivity – $C1a_2$ [m s^{-1}]	4.86×10^{-6}–2.08×10^{-5}	4.05×10^{-6}	4.05×10^{-5}
Saturated conductivity – $C1b$ [m s^{-1}]	4.05–6.02×10^{-6}	3.70×10^{-6}	3.70×10^{-5}
Porosity[a] – $C1a_1$ [–]	0.36–0.49	0.36/0.25/0.25/0.21	0.49/0.44/0.44/0.34
Porosity[a] – $C1a_2$ [–]	0.30–0.46	0.33/0.18/0.18/0.18	0.46/0.41/0.41/0.32
Porosity[a] – $C1b$ [–]	0.23–0.39	0.27/0.13/0.13/0.13	0.39/0.35/0.35/0.27
Air entry value (SWRC)[b] – $C1a_1$ [m]	0.008–0.042	0.042	0.008
Shape factor of the SWRC[b] – $C1a_1$ [–]	12.9–14.7	12.9	14.7
Air entry value (SWRC)[b] – $C1a_2$ [m]	0.035–0.049	0.049	0.035
Shape factor of the SWRC[b] – $C1a_2$ [–]	11.5–13.1	11.5	13.1
Air entry value (SWRC)[b] – $C1b$ [m]	0.016–0.21	0.021	0.016
Shape factor of the SWRC[b] – $C1b$ [–]	12.3–13.7	12.2	13.7

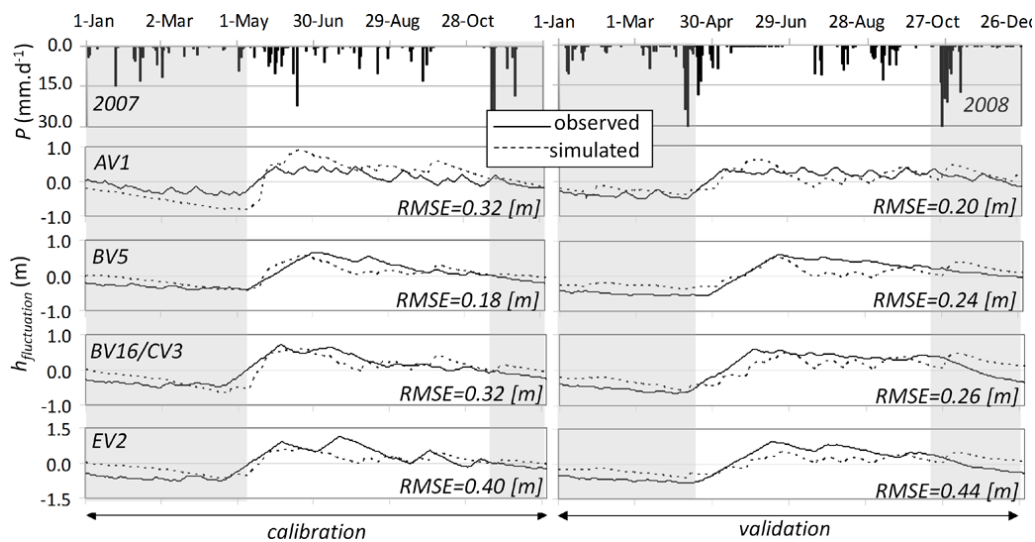[a] Porosity values vary between units U1/U2/U3/U4; [b] values taken from Malet et al. (2005).

Fig. 7. Observed and simulated groundwater level fluctuations over years 2007 (calibration period) and 2008 (validation period) with corresponding root-mean-squares errors values (RMSE). The 0 at the y-axis corresponds to average observed or simulated groundwater level. The shadow areas correspond to the period when the snow cover was observed.

When analysing the differences between the scenarios where fissure network are implemented (scenario-1–2) one can see how the model captures the behaviour of the fissure network. Let us analyse two areas within the landslide (Fig. 8a) being representative for:

– fissure network with limited downslope drainage – area A – located in the upper part of the landslide, where the highest fissure fraction (max $F_{fis} \geq 25\%$) and the highest variability in fissure fraction (max F_{fis} − min F_{fis} up to 10 %) occurs during the simulation period and

– fissure network with relatively unlimited drainage – area B – lower part of the landslide, where fissure fraction is relatively high (F_{fis} from 10 % to 20 %).

The area located just below area A is characterised by relatively limited fissure fraction ($F_{fis} = 5\%$). As a consequence of this set up, the fissure network in the area A behaves as a network of dead-end fissures. The rising saturation of the particular soil column within area A results in rising chance for fissures to be connected (scenario-2). However, with limited drainage possibilities in downstream direction this results in rising of the average groundwater level in the area A (Fig. 10c). When mechanical feedback is included (scenario-1), the increase in the soil column saturation influences the stability of the soil column and therefore fissure volume. Growing volume of fissures (i.e., increase of available water storage) results in lowering of groundwater
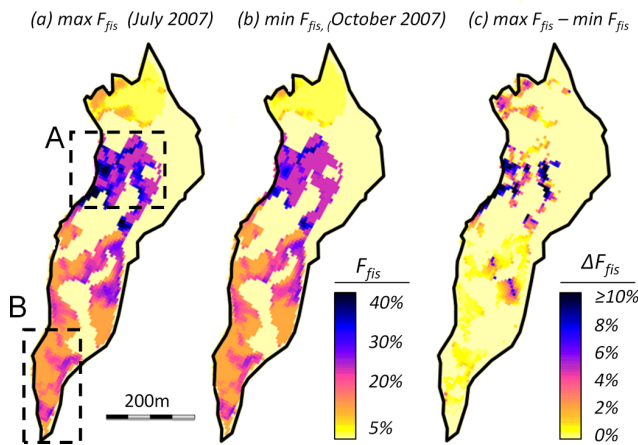
Fig. 8. The modelled dynamics in fissure fraction during: **(a)** maximal fissure fraction (max F_{fis}), **(b)** minimal fissure fraction (min F_{fis}) and **(c)** the difference between two extremes (max F_{fis}-min F_{fis}) that occurs during one year simulation period (2007). The areas A and B indicated in Fig. 7a are further discussed.

level. Nevertheless, the annual average groundwater level in area A simulated with scenario-1 is still higher than the one modelled with scenario-3 (where fissures are not considered). The evidence for dead-end like fissure behaviour at the lower part of area A is: (a) the results of small-sprinkling experiment performed in this area (Krzeminska et al., 2013) showing that infiltration processes are controlled by the extended, but poorly connected fissure network and prolonged periods of elevated pore water pressure are observed after the sprinkling; (b) the observation of saturated tension cracks, with the standing water, observed in this part of the landslide (Malet et al., 2005).

The opposite behaviour is observed in the area B. Here, the modelled fissure network extends till the border of the landslide and can provide natural drainage network when the fissures are connected between adjacent cells. Therefore, even if the average groundwater level in the area increases after introducing fissure network, it decreases when accounting for hydrological and mechanical feedbacks (scenario-1) and there are almost no differences when compared with scenario-3 (where no fissure network is considered). This behaviour is also observed in the field: the average groundwater level observed in the piezometer EV2 is lower than in the middle part of the landslide and it shows moderate piezometric responses.

The results presented herein are, in general, in agreement with previous studies (McDonnell, 1990; Uchida et al., 2001) confirming that presence of fissures influences the percolation processes and storage capacity of the soil. Moreover, they confirm that fissure volume and fissure connectivity control the distribution of soil pore water pressure within the landslide (Cameira et al., 2000; Uchida et al., 2001; Nobles et al., 2004; Krzeminska et al., 2012, 2013). The presence of
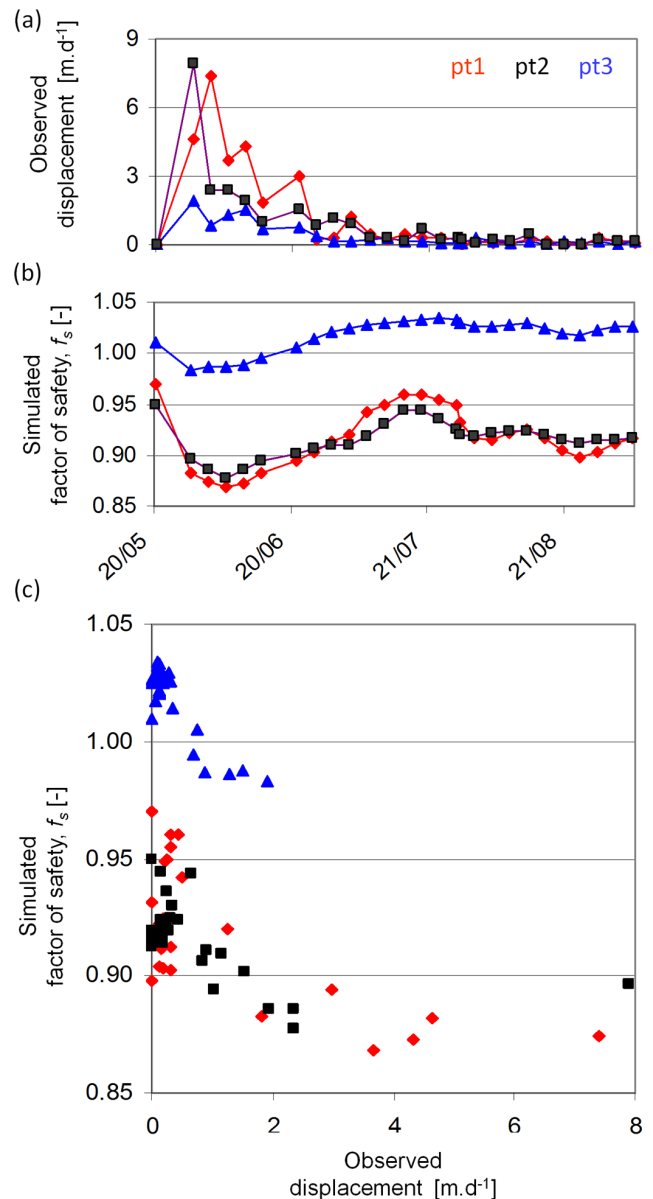

Fig. 9. (a) Observed displacement rates for points pt1, pt2 and pt3 (Travelletti et al., 2012); **(b)** the factor of safety, f_{s}, simulated with additional adjustment of "snow pack/snow melt" model; **(c)** the relationship between the "new" f_{s} and observed displacement rates (Travelletti et al., 2012). For the location of the points see Fig. 3a.

disconnected fissures increases the storage capacity whereas outflow is impeded. This results in persistently high groundwater levels. The presence of connected fissures network shows fast preferential drainage as the dominant process and, thus, results in a lower groundwater level.

Logically, groundwater level behaviour results in analogous differences, between the scenarios, in simulated stability of the particular cells. Implementation of the hydrological and mechanical feedbacks (scenario-1) results in a general increase of stability (f_{s}) when comparing to the scenarios
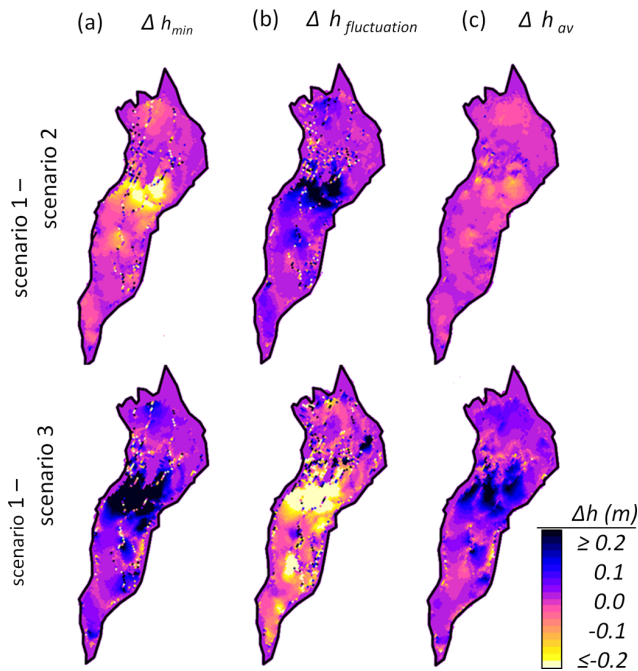
Fig. 10. The simulated groundwater level behaviour – difference between the four scenarios.

Fig. 11. General trends in groundwater level (h_{av}) and local factor of safety (f_{s}) when analysing four scenarios.

where only hydrological feedback is considered to be dynamic (scenario-2) (Fig. 6). The findings are schematically summarised in Fig. 11.

Last, but not least, it is important to stress the main limitation of the proposed model. The model uses the pre-defined landslide geometry that is not changing during the simulation periods and, thus, no mass displacement has been considered. Moreover, the implemented feedbacks in fissures characteristics have no influence on the strength properties of the material. The use of the infinite slope model is also an important simplification and calculated f_{s} represent local conditions only (cell level). However, Milledge et al. (2012) showed that infinite slope model can successfully be applied for landslides with a length/depth ratio of at least 25. The Super-Sauze landslide is a complex slow-moving translational landslide with the length around 900 m and the maximal depth of sliding material approximately 9 m (Malet et al., 2005; Travelletti and Malet, 2012).

Ideally, looking towards the future and drawing on the work presented by Travelletti et al. (2012) and Stumpf et al. (2013), high spatial resolution observation of surface displacement together with detailed observation of dynamic characteristics of fissure patterns should be performed on regular basis giving opportunity to link fissure volume to differential displacement. This would allow us to improve the proposed relationship (Eq. 2) and to take the mechanical basis of fissure appearance into account. Clearly, the empirical relation that is presently used between the local factor of safety and fissure volume is debatable. The excess shear
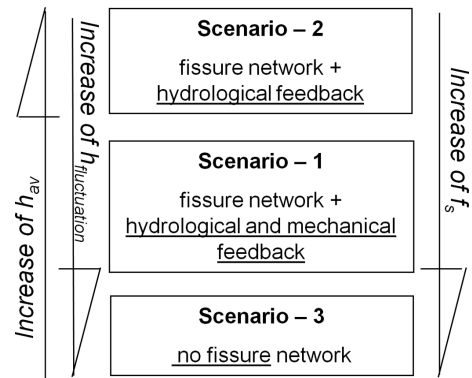
stress could be used to calculate the displacement, but this would add complexity as assumptions on the nature of the displacement have to be taken into account. Still such an approach would not take inter-slice (inter-cell) forces into account and ignore the ensuing mass transfer. The implication is that there is no direct feedback between instability and the driving forces and only the indirect feedback through the fissure-controlled hydrology is taken into account. A comprehensive alternative to address these limitations would be to consider the force differences between cells and make assumptions on the possible compression and dilatation of the soil volume within a cell; volumetric changes can then be logically tied to changes in fissure volume. Essential to include the direct feedback between instability and the driving forces is the incorporation of mass transfer (e.g., as included in the SlowMove model such as presented by Travelletti, 2011). Yet, such a model would require a cumbersome update of the mass of the respective soil constituents and the associated properties and states; such an approach implies mixing to obtain effective, voxel-based parameters, which is at odds with the discrete nature of the fissure network. An improved scheme would, therefore, consider mass transfer and its direct effect on the driving forces through the matrix properties of the soil while the implied changes in the form of dilatation or compression for the current volume would affect the fissure content and nature. In order to keep such a scheme manageable, however, it requires close integration with information from field observations and laboratory tests and consequently is a matter for future studies.

5 Conclusions

This paper describes an initial attempt to model the hydrology of the Super-Sauze landslide with accounting for preferential fissure flow and the dynamically changing characteristics of fissure network. The spatially distributed hydrological and slope stability model (STARWARS) has been adapted to account for geotechnical and hydrological feedbacks on

changes in fissure volume and fissure connectivity (Van Beek, 2002; Krzeminska et al., 2012). The hydrological parameters used for model calibration are taken from the work of Malet et al. (2005).

The model reproduces well the observed hydrological behaviour of the landslide, accounting for spatial differences in hydrological responses and captures all the physical phenomena and their variation in time and space. Our research outlines that fissure volume and fissure connectivity control the distribution of soil pore water pressure within the landslide. Implementation of the dynamic characteristics of fissure network allowed to account for the spatial and temporal variability in the hydrological processes dominating in particular areas of the landslide that are often observed in the field.

It is important to stress that proposed relationships between saturation of the soil column and fissure connectivity and between the mass movement and fissure volume are theoretical only. However, our research indicates the need for further study in the direction of measurement and monitoring of fissures characteristic and their variation over time. This would allow for a better understanding and constrain of the proposed relationship.

Edited by: R. Greco

References

Anderson, T. L.: Fracture Mechanics: Fundamentals and Applications, 3rd Edn., Taylor & Francis, 621 pp., 2005.

Beckers, J. and Alila, Y.: A model of rapid preferential hillslope runoff contributions to peak flow generation in a temperate rain forest watershed, Water Resour. Res., 40, W03501, doi:10.1029/2003WR002582, 2004.

Beven, K. and Germann, P.: Macropores and water flow in soils, Water Resour. Res., 18, 1311–1325, 1982.

Bievre, G., Jongmans, D., Winiarski, T., and Zumbo, V.: Application of geophysical measurements for assessing the role of fissures in water infiltration within a clay landslide (Trieves area, French Alps), Hydrol. Process., 26, 2128–2142, doi:10.1002/hyp.7986, 2011.

Bogaard, T. A.: Analysis of hydrological processes in unstable clayey slopes, PhD Thesis, University of Utrecht, Netherlands, 2001.

Bogaard, T. A.: A state-dependent ground water recharge model for landslide research, Proc. 9th Int. Cong. IAEG, Durban, South Africa, 1489–1496, 2002.

Cameira, M. R., Ahuja, L., Fernando, R. M., and Pereira, L. S.: Evaluating field-measured soil hydraulic properties in water transport simulations using the RZWQM, J. Hydrol, 236, 78–90, 2000.

Fannin, R. J., Jaakkola, J., Wilkinson, J. M. T., and Hetherington, E. D.: Hydrologic response of soils to precipitation at Carnation Creek, British Columbia, Canada, Water Resour. Res., 36, 1481–1494, 2000.

Farrel, D. and Larson, W.: Modeling of the pore structure of porous media, Water Resour. Res., 8, 699–705, 1972.

Gerke, H. H.: Preferential flow descriptions for structured soils, J. Plant Nutr. Soil Sc., 169, 382–400, 2006

Greco, R.: Preferential flow in macroporous swelling soil with internal catchment: model development and applications, J. Hydrol., 269, 150–168, 2002.

Gwo, J. P., Jardine, P. M., Wilson, G. V., and Yeh, G. T.: A multiple-pore-region concept to modelling mass transfer in subsurface media, J. Hydrol., 164, 217–237, 1995.

Jarvis, N. J.: A review of non-equilibrium water flow and solute transport in soil macropores: principles, controlling factors and consequences for water quality, Eur. J. Soil Sci., 58, 523–546, 2007.

Kosugi, K., Uchida, T., and Mizuyama, T.: Numerical calculation of soil pipe flow and its effect on water dynamics in a slope, Hydrol. Process., 18, 777–789, 2004.

Krzeminska, D. M., Bogaard, T. A., van Asch, Th. W. J., and van Beek, L. P. H.: A conceptual model of the hydrological influence of fissures on landslide activity, Hydrol. Earth Syst. Sci., 16, 1561–1576, doi:10.5194/hess-16-1561-2012, 2012.

Krzeminska, D. M., Bogaard, T. A., Debieche, T.-H., Marc, V., and Malet, J.-P.: Sprinkling tests to understand hydrological behaviour of mudslide, Proc. Int. Conf. "The Second World Landslide Forum", Rome, Italy, in press, 2013.

Lindenmaier, F.: Hydrology of a large unstable hillslope at Ebnit, Vorarlberg: identifying dominating processes and structures, PhD Thesis, Universität Potsdam, Germany, 2007.

Malet, J.-P.: Les glissements de type écoulement dans les marnes noires des Alpes de Su. Morphologie, fonctionnement et modélisation hydromécanique, PhD Thesis, Université Louis Pasteur, Strasbourg, 2003.

Malet, J.-P., Maquaire, O., and Calais, E.: The use of Global Positioning System techniques for the continuous monitoring of landslides: application to the Super-Sauze earthflow (Alpes-de-Haute-Provence, France), Geomorphology, 43, 33–54, 2002.

Malet, J.-P., Auzet, A.-V., Maquaire, O., Ambroise, B., Descroix, L., Esteves, M., Vandervaere, J.-P., and Truchet, E.: Soil surface characteristics influence on infiltration in black marls: application to the Super-Sauze earthflow (Southern Alps, France), Earth Surf. Proc. Land., 28, 547–564, 2003.

Malet, J.-P., van Asch, Th. W. J., van Beek, R., and Maquaire, O.: Forecasting the behaviour of complex landslides with a spatially distributed hydrological model, Nat. Hazards Earth Syst. Sci., 5, 71–85, doi:10.5194/nhess-5-71-2005, 2005.

McDonnell, J. J.: The influence of macropores on debris flow initiation, Q. J. Eng. Geol. Hydroge., 23, 325–331, doi:10.1144/GSL.QJEG.1990.023.04.06, 1990.

Milledge, D. G., Griffiths, D. V., Lane, S. N., and Warburton J.: Limits on the validity of infinite length assumptions for modelling shallow landslides, Earth Surf. Proc. Land., 37, 1158–1166, doi:10.1002/esp.3235, 2012.

Millington, R. J. and Quirk, J. P.: Permeability of porus media, Nature, 183, 387–388, 1959.

Mulungu, D. M. M., Ichikawa, Y., and Shiiba, M.: A physically based distributed subsurface-surface flow dynamics model for forested mountainous catchments, Hydrol. Process., 19, 3999–4022, 2005.

Niethammer, U., James, M. R., Rothmund, S., Travelletti, J., and Joswig, M.: UAV-based remote sensing of the Super-Sauze landslide: evaluation and results, Eng. Geol., 128, 2–11, 2012.

Nobles, M. M., Wilding, L. P., and McInnes, K. J.: Pathways of dye tracer movement through structured soils on a macroscopic scale, Soil Sci., 169, 229–242, 2004.

Noguchi, S., Tsuboyama, Y., Sidle, R. C., and Hosoda, I.: Morphological characteristics of macropores and the distribution of preferential flow pathways in a forested slope segment, Soil Sci. Soc. Am. J., 63, 1413–1423, 1999.

Schulson, E. M. and Duval, P.: Creep and Fracture of Ice, Cambridge University Press, New York, 2009.

Sidle, R. C., Tsuboyama, Y., Noguchi, S., Hosada, I., Fujieda, M., and Shimizu, T.: Stormflow generation in steep forested headwaters: a linked hydrogeomorphic paradigm, Hydrol. Process., 14, 369–385, 2000.

Šimůnek, J., Jarvis, N. J., Van Genuchten, M. T., and Gardenas, A.: Review and comparison of models for describing non-equilibrium and preferential flow and transport in the vadose zone, J. Hydrol., 272, 14–35, 2003.

Skempton, A. W.: The long-term stability of clay slopes, Geotechnique, 14, 95–102, 1964.

Stumpf, A., Malet, J.-P., Kerle, N., Niethammer, U., and Rothmund, S.: Image-based mapping of surface fissures for the investigation of landslide dynamics, Geomorphology, 186, 12–27, doi:10.1016/j.geomorph.2012.12.010, 2013.

Travelletti, J.: Imagerie multi-paramètres et multi-résolutions pour l'observation et la caractérisation des mécanismes de glissements-coulées, PhD Thesis, University of Caen, France, 2011.

Travelletti, J. and Malet, J.-P.: Characterisation of the 3D geometry of flow-like landslides: A methodology based on the integration of heterogeneous multi-source data, Eng. Geol., 128, 30–48, 2012.

Travelletti, J., Delacourt, C., Allemand, P., Malet, J.-P., Schmittbuhl, J., Toussaint, R., and Bastard, M.: Correlation of multi-temporal ground-based optical images for landslide monitoring: application, potential and limitations, Journal of Photogrammetry and Remote Sensing, 70, 39–55, 2012.

Tsuboyama, Y., Sidle, R. C., Noguchi, S., and Hosada, I.: Flow and transport through the soil matrix and macropores of hillslope segment, Water Resour. Res., 30, 879–890, 1994.

Uchida, T., Kosugi, K., and Mizuyama, T.: Effects of pipeflow on hydrological process and its relation to landslide: a review of pipeflow studies in forested headwater catchments, Hydrol. Process., 15, 2151–2174, 2001.

Van Asch, T. W. J., Hendriks, M. R., Hassel, R., and Rappange, F. E.: Hydrological triggering conditions of landslide in varved clays in the French Alps, Eng. Geol., 42, 239–251, 1996.

Van Asch, T. W. J., Van Dijk, S. J. E., and Hendriks, M. R.: The role of the overland flow and subsurface flow on spatial distribution of soil moisture in the top soil, Hydrol. Process., 15, 2325–2340, 2001.

Van Asch, T. W. J., Van Beek, L. P. H., and Bogaard, T. A.: Problems in predicting the mobility of slow-moving landslides, Eng. Geol., 91, 46–55, 2007.

Van Beek, L. P. H.: Assessment of the influence of changes in land use and climate on landslide activity in a Mediterranean environment, PhD Thesis, University of Utrecht, Netherlands, 2002.

Van Beek, L. P. H. and Van Asch, T. W. J.: A combined conceptual model for the effects of fissure-induced infiltration on slope stability, in: Process Modelling and Landform Evolution, Lect. Notes Earth Sci., 78, 147–167, doi:10.1007/BFb0009716, 1999.

Van Beek, L. P. H. and Van Asch, Th. W. J.: Regional assessment of the effects of land-use change on landslide hazard by means of physically based modelling, Nat. Hazards, 31, 289–304, 2004.

Van Schaik, L.: The role of macropore flow from plot to catchment scale. A study in a semi-arid area, PhD Thesis, University of Utrecht, Netherlands, 2010.

Walter, M., Arnhardt, C., and Joswig, M.: Seismic monitoring of rockfalls, slide quakes, and fissure development at the Super-Sauze mudslide, French Alps, Eng. Geol., 128, 12–22, 2012.

Weiler, M. and McDonnell, J. J.: Conceptualizing lateral preferential flow and flow networks and simulating the effects on gauged and ungauged hillslopes, Water Resour. Res., 43, W03403, doi:10.1029/2006WR004867, 2007.

Zehe, E. and Blöschl, G.: Predictability of hydrologic response at the plot and catchment scales – the role of initial conditions, Water Resour. Res., 40, W10202, doi:10.1029/2003WR002869, 2004.

Zhang, G. P., Savenije, H. H. G., Fenicia, F., and Pfister, L.: Modelling subsurface storm flow with the Representative Elementary Watershed (REW) approach: application to the Alzette River Basin, Hydrol. Earth Syst. Sci., 10, 937–955, doi:10.5194/hess-10-937-2006, 2006.